Aluminum−Nitrogen Rings and Cages with Organic Handles: A Theoretical Study

Cong Trinh,[†] Alexey Y. Timoshkin,*[,†] and Gernot Frenking[‡]

Inorganic Chemistry Group, Department of Chemistry, St. Petersburg State University, University Pr. 26, Old Peterhof 198504, Russia, and Philipps-Universität Marburg, Hans-Meerwein-Strasse, D-35032 Marburg, Germany

Received: July 4, 2008; Revised Manuscript Received: January 2, 2009

The structures and stability of monomeric and oligomeric compounds resulting from the elimination of 2 mol of HBr from the $AlBr_3$en complex have been studied theoretically at the B3LYP/LANL2DZ(d,p) level of theory. Two series of the ring and cage oligomer compounds were considered: imino $[AlBrNCH_2CH_2NH_2]_n$, $n = 1-4, 6$ (**I**$_n$), and isomeric amido $[\overline{AlBrNHCH_2CH_2NH}]_n$, $n = 1-3$ (**A′**$_n$), species. In all cases the amido isomers are 95−295 kJ mol^{-1} more stable compared to their imino counterpairs. Intramolecular donor−acceptor interactions play an important role in the stabilization of the structure. Possible pathways of the polymerization have also been explored. Although the generation of the oligomers via HBr elimination in the gas phase is predicted to be thermodynamically unfavorable, operation of such reactions in the condensed phase is feasible. Substitution of bromine by hydrogen makes H_2 elimination reactions thermodynamically favorable. This opens a perspective for the synthesis of novel ladder-type oligomers with a continuous $(AlN)_n$ core supported by C_2H_4 balustrade and imino cages with C_2H_4 handles.

1. Introduction

Group 13−15 binary compounds serve as UV photodetectors, light-emitting diodes, solar cell elements, advanced ceramic materials, and chemical sensors.[1] Chemical vapor deposition (CVD)[2,3] is one of the leading methods for the production of group 13−15 materials. In recent years, fabrication of one-, two-, and three-dimensional group 13−15 nanoarchitectures as a result of chemical reactions has attracted the attention of chemists. Examples on the growth of the group 13−15 nanostructures include controlled gas-phase growth of one-dimensional AlN structures in the aluminum−ammonia system.[4] While the exact mechanism of the process is not fully understood, it is believed that polymeric (oligomeric) species may play an important role. Very recently, pyrolysis of the donor−acceptor-stabilized trisaminoalane $Me_3N-Al[N(H)Dipp]_3$ (Dipp = 2,6-^{i}PrC_6H_3) yielded aluminum−nitrogen oligomers which were converted to AlN in an ammonia atmosphere.[5] Conversion of organometallic imino cages to AlN was reported by Koyama et al.[6] and highlighted in a review by Mori and Sugahara.[7] Mixed poly(alkyliminoalane)s $[HAlNR]_n$ (R = allyl, ethyl) have been synthesized and successfully converted into AlN.[8] It is argued that cross-linking reactions play a role in this conversion.[8] Possible pathways of formation of 2D AlN structures were considered in detail by Himmel[9] using theoretical methods.

Recently, donor−acceptor (DA) complexes of group 13 metal trihalides MX_3 with N-containing bidentate donors attracted our attention as potential precursors for the synthesis of group 13 composite nitrides.[10,11] Systematic theoretical studies of the dissociation and HX elimination reactions from complexes of MX_3 (M = Al,Ga; X = Cl, Br, I) with ethylenediamine (en) were performed.[12] We experimentally observed that on heating M_2X_6en complexes (M = Al,Ga; X = Cl, Br, I) eliminate HX and form associates with high molecular weight (600−900 amu).[11] For the Al_2Br_6en system, for which in the gas phase the formation of high mass species with high molecular weight was found the most abundant, we also reported a theoretical study of the structures and stabilities of source DA complexes and products resulting from elimination of 1 mol of HBr.[11] In the present paper, we systematically explore with theoretical methods the structures and stability of imino species resulting from elimination of 2 mol of HBr from the $AlBr_3$en complex. Such compounds and their derivatives are potential precursors for the controlled synthesis of AlN.[13] Since the $\overline{AlBr_2NHC_2H_4NH_2}$ (**$_{ring}$A**) structure was previously identified as one of the key decomposition products,[11] in the present work we considered the **$_{ring}$A** compound as a starting point for the next HBr elimination and subsequent oligomerization reactions (Scheme 1).

Following the notations from our previous papers,[11,12] in this paper **I** indicates the monomeric imino compound $AlBrNCH_2CH_2NH_2$ and its respective oligomers with oligomerization degree n are denoted **I**$_n$. The isomeric amido structure $\overline{AlBrNHCH_2CH_2NH}$ is denoted as **A′** and respective oligomers are denoted as **A′**$_n$. Several isomers for each compound have been considered which are distinguished by subscript symbols **a**, **b**, etc.

2. Computational Details

The Gaussian03 program package[14] was used throughout. The geometries were fully optimized using density functional theory (DFT) with the B3LYP[15,16] hybrid functional in conjunction with the effective core potential basis set LANL2DZ[17] augmented by d and p polarization functions as described in ref 18. The previous study of complexes of group 13 metal halides with ammonia at B3LYP/LANL2DZ(d,p) showed satisfactory agreement with high-temperature experimental data.[18] As confirmed by analytical evaluation of the second derivatives, all structures reported here are minima on the potential energy surface.

* To whom correspondence should be addressed. Fax: +7(812)428-6939. E-mail: alextim@AT11692.spb.edu.
[†] St. Petersburg State University.
[‡] Philipps-Universität Marburg.

10.1021/jp805904e CCC: $40.75
Published on Web 03/11/2009

SCHEME 1: Processes of HBr Elimination from $_{ring}$A Leading to Imino and Amido Oligomers and Polymers

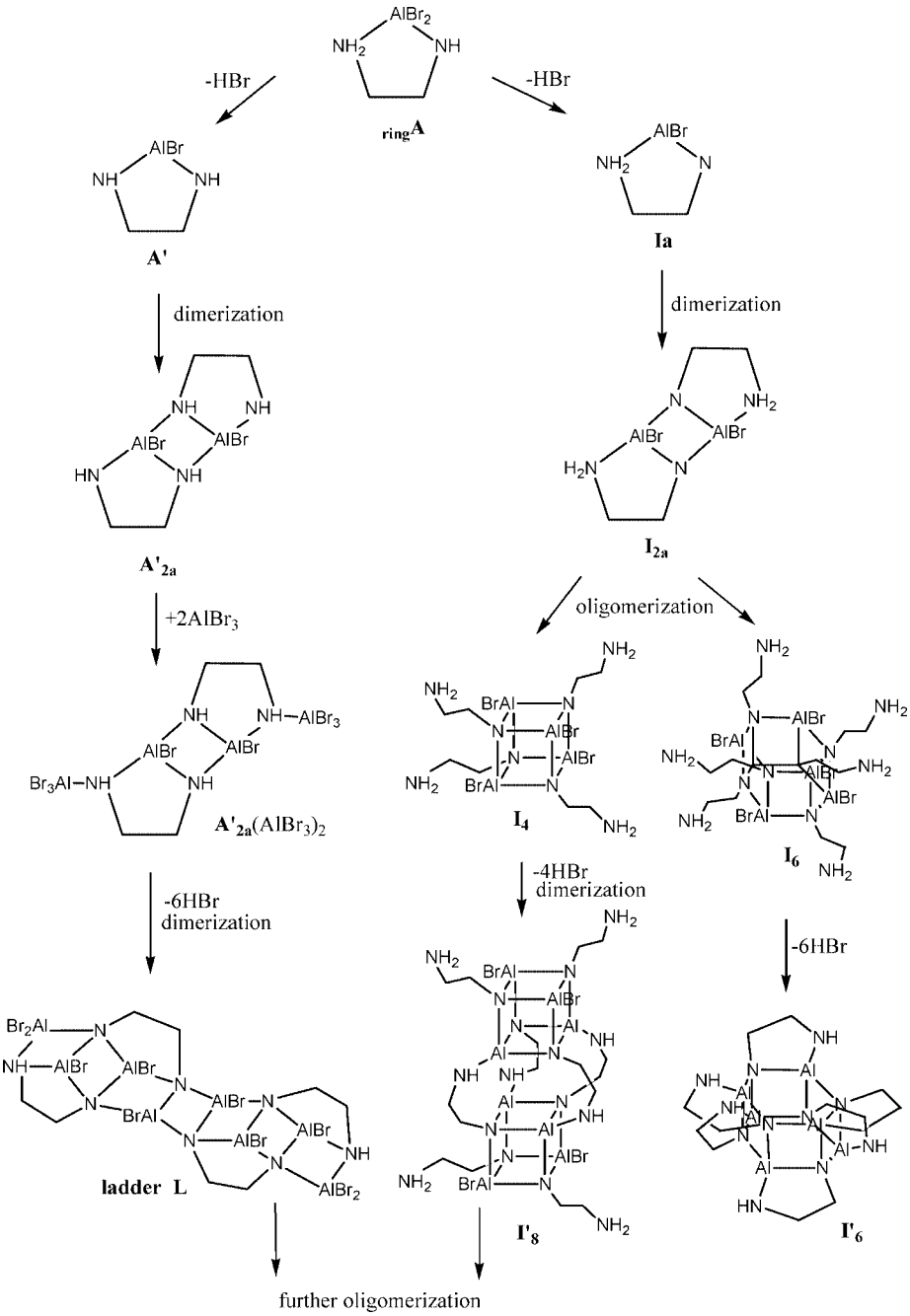

Standard enthalpies were evaluated taking into account zero-point vibrational energy and thermal corrections using the rigid rotor−harmonic oscillator approximation.

3. Results and Discussion

3.1. Oligomerization of Imino Compounds (I_n Series). We start our discussion with the imino species, featuring a mono-substituted nitrogen atom bonded to aluminum. The optimized structures of $\mathbf{I_n}$ species are given in Figure 1. For monomeric $BrAlNC_2H_4NH_2$, the asymmetric ring isomer $\mathbf{I_a}$ (Figure 1a) is 89 kJ mol^{-1} more stable compared to the C_s-symmetric chain isomer $\mathbf{I_b}$ (Figure 1b). The cyclic structure $\mathbf{I_a}$ is stabilized by an intramolecular DA interaction with its own substituent. DA-supported $\mathbf{I_a}$ has an Al−N distance of 1.709 Å, which is considerably longer compared to the distance in unsupported $\mathbf{I_b}$ (1.648 Å). The latter value is close to that predicted for monomeric BrAlNH (1.652 Å [19]). These observations indicate that substitution of H by the nonchelating $-C_2H_4NH_2$ group only marginally affects the Al−N bond distances, while chelating ligands lengthen the Al−N bond distance by about 0.06 Å.

Since both $\mathbf{I_a}$ and $\mathbf{I_b}$ structures feature aluminum and nitrogen atoms with low coordination numbers, oligomerization of such compounds is expected to be favorable. We considered three isomers of $\mathbf{I_2}$ dimers. Their optimized structures are given in Figures 1c−e. All three isomers possess a planar Al_2N_2 ring. In the C_i-symmetric structure $\mathbf{I_{2a}}$, originating from the ring monomer $\mathbf{I_a}$, the aluminum atoms attain the favorable coordination number 4. As a result, this isomer is 172 kJ mol^{-1} more stable than the energetically nearly degenerate structures $\mathbf{I_{2b}}$ and $\mathbf{I_{2c}}$ constructed by dimerization of the chain monomer $\mathbf{I_b}$. The structure $\mathbf{I_{2b}}$ is only 0.1 kJ mol^{-1} more stable compared to $\mathbf{I_{2c}}$.

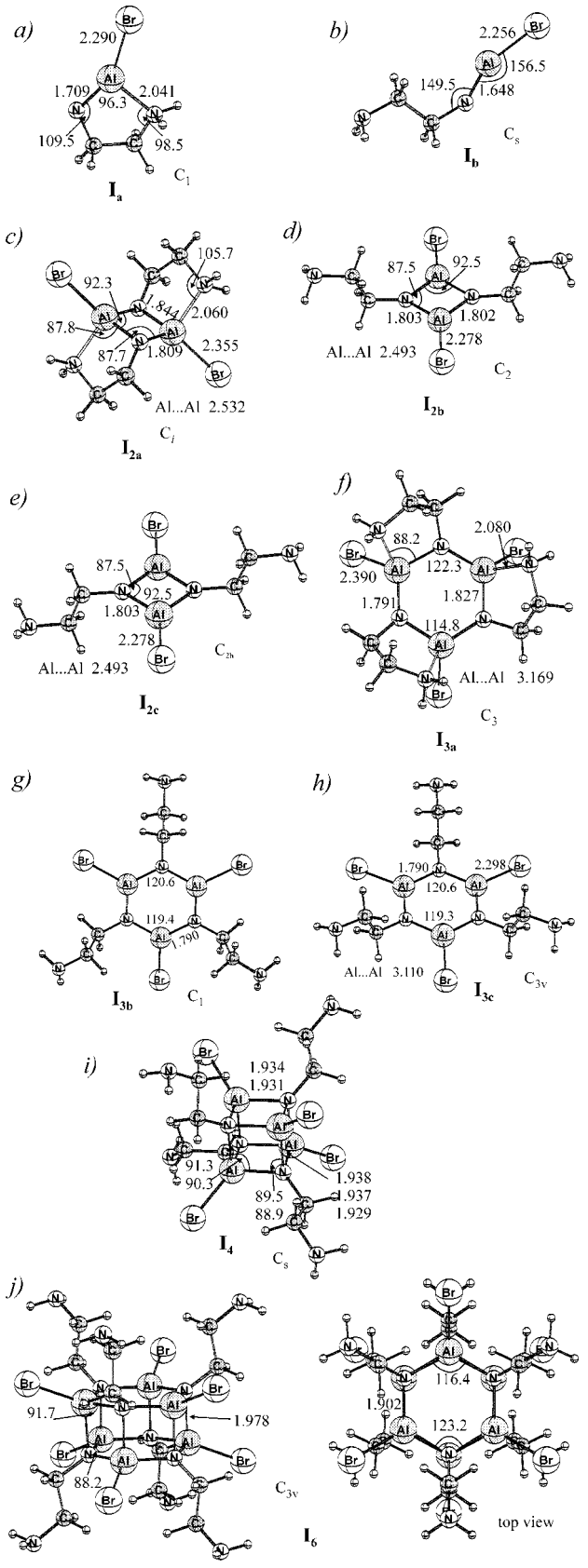

Figure 1. Optimized structures of imino compounds $\mathbf{I}_n$ (B3LYP/LANL2DZ(d,p) level of theory): (a) ring isomer of the monomeric imino compound ($\mathbf{I_a}$); (b) chain isomer of the monomeric imino compound ($\mathbf{I_b}$); (c) ring isomer of the imino dimer ($\mathbf{I_{2a}}$); (d) chain isomer of the imino dimer ($\mathbf{I_{2b}}$); (e) chain isomer of the imino dimer ($\mathbf{I_{2c}}$); (f) ring isomer of the imino trimer ($\mathbf{I_{3a}}$); (g) chain isomer of the imino trimer ($\mathbf{I_{3b}}$); (h) chain isomer of the imino trimer ($\mathbf{I_{3c}}$); (i) imino tetramer ($\mathbf{I_4}$); (j) imino hexamer ($\mathbf{I_6}$).

The Al−N bond distance of 1.803 Å in $\mathbf{I_{2b}}$ corresponds well with the value of 1.801 Å predicted for $[BrAlNH]_2$.[19] The additional intramolecular DA interaction in $\mathbf{I_{2a}}$ lengthens the Al−N bonds in the Al_2N_2 cycle and makes them strongly unequivalent: 1.809 and 1.844 Å. The longer Al−N distance occurs with the bridging $-C_2H_4NH_2$ group presumably due to the additional strain associated with AlN_2C_2 ring closure.

The trimeric compounds follow the same pattern as found for the dimers. The intramolecular DA-supported structure $\mathbf{I_{3a}}$ (Figure 1f) is 228 kJ mol^{-1} more stable than the unsupported isomers $\mathbf{I_{3b}}$ and $\mathbf{I_{3c}}$ (Figure 1g,h). One can observe that upon an increase of the oligomerization degree n the Al−N bond lengthening due to DA stabilization decreases by 0.061, 0.042, and 0.037 Å for $n = 1$, 2, and 3, respectively, in accord with the calculated decrease in the relative stability of the isomers (89, 86, and 76 kJ mol^{-1} per mole of monomeric unit for $n = 1$, 2, and 3, respectively).

The dimeric $\mathbf{I_{2b,c}}$ and trimeric $\mathbf{I_{3b,c}}$ rings still possess unsaturated Al atoms with coordination number 3, which are capable of further interactions. There are two possible ways of achieving the coordination number 4. The first one is an intramolecular DA stabilization which leads to cyclization toward $\mathbf{I_{2a}}$ and $\mathbf{I_{3a}}$. Alternatively, stabilization of the DA "unsupported" $\mathbf{I_{2b,c}}$ and $\mathbf{I_{3b,c}}$ rings may be achieved by dimerization and formation of cubane and drum-type cages $\mathbf{I_4}$ and $\mathbf{I_6}$. The optimized structures of such cages are presented in parts i and j, respectively, of Figure 1. The values of intramolecular donor−acceptor stabilization enthalpies for $\mathbf{I_{2b}} \rightleftarrows \mathbf{I_{2a}}$ and $\mathbf{I_{3b}} \rightleftarrows \mathbf{I_{3a}}$ are −168 and −223 kJ mol^{-1}, respectively. They are less exothermic compared to the dimerization of $\mathbf{I_{2b}}$ and $\mathbf{I_{3b}}$ (standard enthalpies for processes $\mathbf{I_{2b}} \rightleftarrows {}^1/_2\mathbf{I_4}$ and $\mathbf{I_{3b}} \rightleftarrows {}^1/_2\mathbf{I_6}$ are −220 and −230 kJ mol^{-1}, respectively). The latter values are close to those predicted for the dimerization of the hydrogen-substituted analogues $[BrAlNH]_2$ and $[BrAlNH]_3$ (−243 and −255 kJ mol^{-1}, respectively).[19] Thus, dimerization of $\mathbf{I_{2b}}$ and $\mathbf{I_{3b}}$ with formation of $\mathbf{I_4}$ and $\mathbf{I_6}$ is energetically more favorable than the intramolecular donor−acceptor stabilization with formation of $\mathbf{I_{2a}}$ and $\mathbf{I_{3a}}$. Therefore, a conversion of the DA-stabilized dimer $\mathbf{I_{2a}}$ into $\mathbf{I_4}$ and DA-stabilized trimer $\mathbf{I_{3a}}$ into $\mathbf{I_6}$ is exothermic but unfavorable by entropy (Table 1).

We conclude that for the imino series $\mathbf{I_n}$ there is a strong tendency toward oligomerization processes. The formation of $\mathbf{I_4}$ and $\mathbf{I_6}$ species with high oligomerization degrees is exothermic, in contrast to amido compounds, where only dimeric and trimeric species were found to be important.[11,20]

Considering the further reactivity of $\mathbf{I_4}$ and $\mathbf{I_6}$, it should be noted that these compounds have four ($\mathbf{I_4}$) or six ($\mathbf{I_6}$) nitrogen atoms capable of additional DA interactions with acceptor molecules. Thus, they can potentially serve as starting compounds for constructing nanosized Al−N-based inorganic−organic polymers. $\mathbf{I_4}$ and $\mathbf{I_6}$ can also undergo self-interaction reactions via HBr elimination. Both intermolecular and intramolecular HBr elimination processes are theoretically possible.

As an example of the intermolecular process, we considered the dimerization of two $\mathbf{I_4}$ cubanes via HBr elimination. The optimized structure of the resulting compound $\mathbf{I'_8}$ is given in Figure 2a. Subsequent repetition of this process will eventually lead to the bromine-free hybrid inorganic−organic $[Al_4N_4(C_2H_4NH)_4]_n$ polymers.

As an example of the intramolecular process, we considered HBr elimination from $\mathbf{I_6}$ with closure into S_6-symmetric six-handle drum $\mathbf{I'_6}$ (Figure 2b). This compound is a very interesting potential precursor to AlN because all aluminum atoms in this structure are bound only to nitrogen atoms. It is expected that

TABLE 1: Thermodynamic Characteristics for the Isomerization and Oligomerization Gas-Phase Reactions[a]

process	$\Delta H°_{298}$, kJ mol^{-1}	$\Delta S°_{298}$, J mol^{-1} K^{-1}	$\Delta G°_{298}$, kJ mol^{-1}	$T_{K=1}$, K
$\mathbf{A'} \rightleftarrows {}^1/_2\mathbf{A'_{2a}}$	−135.3	−95.5	−106.9	1417
${}^1/_2\,\mathbf{A'_{2a}} \rightleftarrows {}^1/_3\mathbf{A'_{3a}}$	−13.8	−31.4	−4.5	440
$\mathbf{A'_{2a}} + 2AlBr_3 \rightleftarrows \mathbf{A'_{2a}}(AlBr_3)_2$	−298.1	−326.8	−200.7	912
$2\mathbf{A'_{2a}}(AlBr_3)_2 \rightleftarrows \mathbf{L} + 6HBr$	811.1	577.0	639.1	1406
$\mathbf{I_a} \rightleftarrows {}^1/_2\mathbf{I_{2a}}$	−280.3	−100.6	−250.4	2787
${}^1/_2\mathbf{I_{2a}} \rightleftarrows {}^1/_3\mathbf{I_{3a}}$	−40.6	−29.1	−31.9	1394
$\mathbf{I_b} \rightleftarrows {}^1/_2\mathbf{I_{2b}}$	−284.7	−95.4	−256.3	2985
$\mathbf{I_{2b}} \rightleftarrows {}^1/_2\mathbf{I_4}$	−220.1	−145.9	−176.6	1508
$\mathbf{I_{3b}} \rightleftarrows {}^1/_2\mathbf{I_6}$	−230.3	−179.6	−176.8	1282
$\mathbf{I_b} \rightleftarrows \mathbf{I_a}$	−88.4	−37.4	−77.3	2366
$\mathbf{I_{2b}} \rightleftarrows \mathbf{I_{2a}}$	−168.2	−72.3	−146.6	2325
$\mathbf{I_{3b}} \rightleftarrows \mathbf{I_{3a}}$	−222.5	−89.2	−195.9	2495
$\mathbf{I_{2a}} \rightleftarrows {}^1/_2\mathbf{I_4}$	−52.0	−60.7	−33.9	856
$\mathbf{I_{3a}} \rightleftarrows {}^1/_2\mathbf{I_6}$	−7.8	−90.4	19.1	86
${}^1/_4\mathbf{I_4} \rightleftarrows {}^1/_6\mathbf{I_6}$	−17.2	−28.9	−8.6	596
$\mathbf{I_6} \rightleftarrows \mathbf{I'_6} + 6HBr$	619.5	752.7	395.1	823
$2\mathbf{I_4} \rightleftarrows \mathbf{I'_8} + 4HBr$	417.2	263.9	338.5	1581
$2\mathbf{A'_{3a}} \rightleftarrows \mathbf{I'_6} + 6HBr$	806.9	599.2	628.3	1347

[a] B3LYP/LANL2DZ(d,p) level of theory.

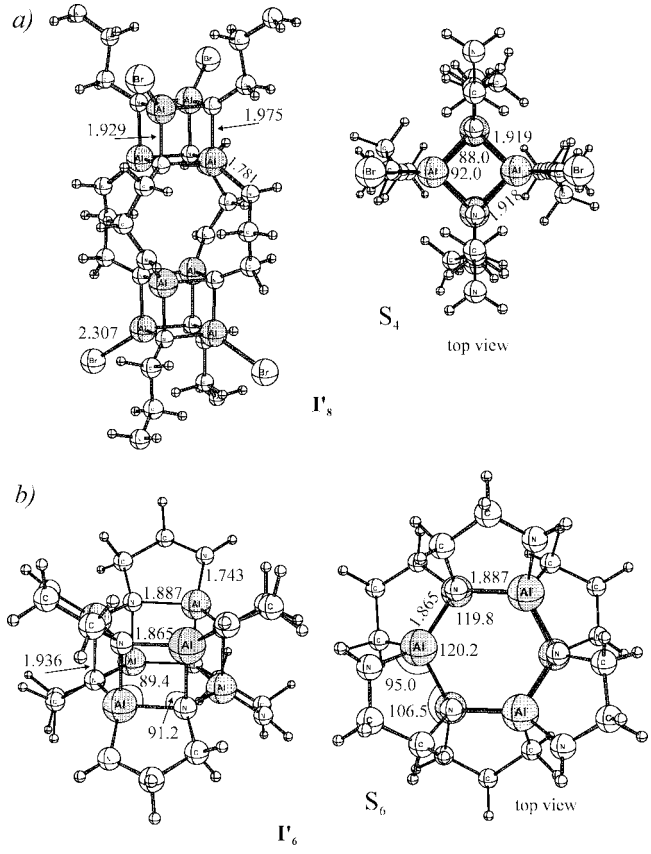

Figure 2. Optimized structures of oligomer compounds: (a) $\mathbf{I'_8}$; (b) six-handle drum $\mathbf{I'_6}$. All distances are in angstroms and all angles in degrees.

cleavage of the carbon-containing "handles" can be achieved in a hydrogen- or an ammonia-rich atmosphere. Since there are no Al−C and Al−Br bonds in $\mathbf{I'_6}$, one can expect that upon its conversion to AlN carbon and halogen contamination could be avoided. The closed-type structure of $\mathbf{I'_6}$ also suggests that this cluster may have significant volatility for practical applications.

3.2. Oligomerization of Imino Compounds ($\mathbf{A'_n}$ Series). Monomeric $\mathbf{A'}$ (Figure 3a) is an isomer of imino compounds $\mathbf{I_a}$ and $\mathbf{I_b}$, and it is 204.9 kJ mol^{-1} more stable than $\mathbf{I_a}$ due to the fact that both Al and nitrogen atoms attain the coordination number 3. The Al−N bond distance in $\mathbf{A'}$ (1.768 Å) is typical for amido compounds (the predicted Al−N distance for Br_2AlNH_2 is 1.755 Å[21]).

Subsequent dimerization of $\mathbf{A'}$ leads to the $\mathbf{A'_{2a}}$ and $\mathbf{A'_{2b}}$ dimers (Figure 3b,c). The C_i-symmetric structure $\mathbf{A'_{2a}}$ with *trans*-orientation of the terminal groups with respect to the Al_2N_2 plane is 5.5 kJ mol^{-1} more stable than asymmetric $\mathbf{A'_{2b}}$ and 117.2 kJ mol^{-1} more stable than the respective imino dimer $\mathbf{I_{2a}}$. For the trimers, the C_3-symmetric structure $\mathbf{A'_{3b}}$ with *syn*-orientation of the Br atoms with respect to the Al_3N_3 ring (Figure 3e) is 9.2 kJ mol^{-1} less stable than the asymmetric *trans*-isomer $\mathbf{A'_{3a}}$ (Figure 3d). The Al_3N_3 rings in these amido trimers are not planar, and the asymmetric *trans*-isomer has better chances for ring relaxation. In general, the structures of the amido dimers and trimers are similar to those theoretically predicted for other group 13−15 amido rings (for a review, see ref 20). $\mathbf{A'_{3a}}$ is also 95.5 kJ mol^{-1} more stable compared to the respective imino trimer $\mathbf{I_{3a}}$.

In agreement with previous findings for amido systems,[20] dimer−trimer reorganization ${}^1/_2\mathbf{A'_{2a}} \rightleftarrows {}^1/_3\mathbf{A'_{3a}}$ is only marginally favorable energetically and unfavorable by entropy. Thus, the $\mathbf{A'_{3a}}$ trimer is predicted to be favorable only at temperatures below 440 K. At higher temperatures, dimeric $\mathbf{A'_{2a}}$ is the most stable gas-phase compound in the $\mathbf{A'_n}$ series.

We also considered the further reactivity of $\mathbf{A'_{2a}}$ and $\mathbf{A'_{3a}}$. Dimerization of $\mathbf{A'_{3a}}$ with elimination of six HBr molecules leads to formation of the "six-handle" drum $\mathbf{I'_6}$ (Figure 2b). Note that $\mathbf{I'_6}$ can also be produced as a result of the intramolecular HBr elimination from the imino cage $\mathbf{I_6}$ (vide supra).

Since $\mathbf{A'_{2a}}$ possesses two nitrogen atoms which are potentially active as Lewis bases, its complexation with two $AlBr_3$ molecules is possible. As expected, complex formation is strongly exothermic but entropically unfavorable (Table 1). The resulting $\mathbf{A'_{2a}}(AlBr_3)_2$ complex (Figure 3f) can undergo further HBr elimination with formation of yet higher oligomers. As an example of such a process, we considered the reaction between two $\mathbf{A'_{2a}}(AlBr_3)_2$ units with elimination of six HBr molecules and formation of a ladder-type structure $\mathbf{L}$ (Figure 3g). Such ladder-type polymers and their functionalized derivatives could find applications as materials for future technologies.

3.3. Thermodynamics of the Reactions Starting from $_{ring}\mathbf{A}$. The general reaction sequence of selected processes starting from $_{ring}\mathbf{A}$ leading to polymers is presented in Scheme 1. Both $\mathbf{I_a}$ and $\mathbf{A'}$ originate from the intramolecular donor−acceptor-

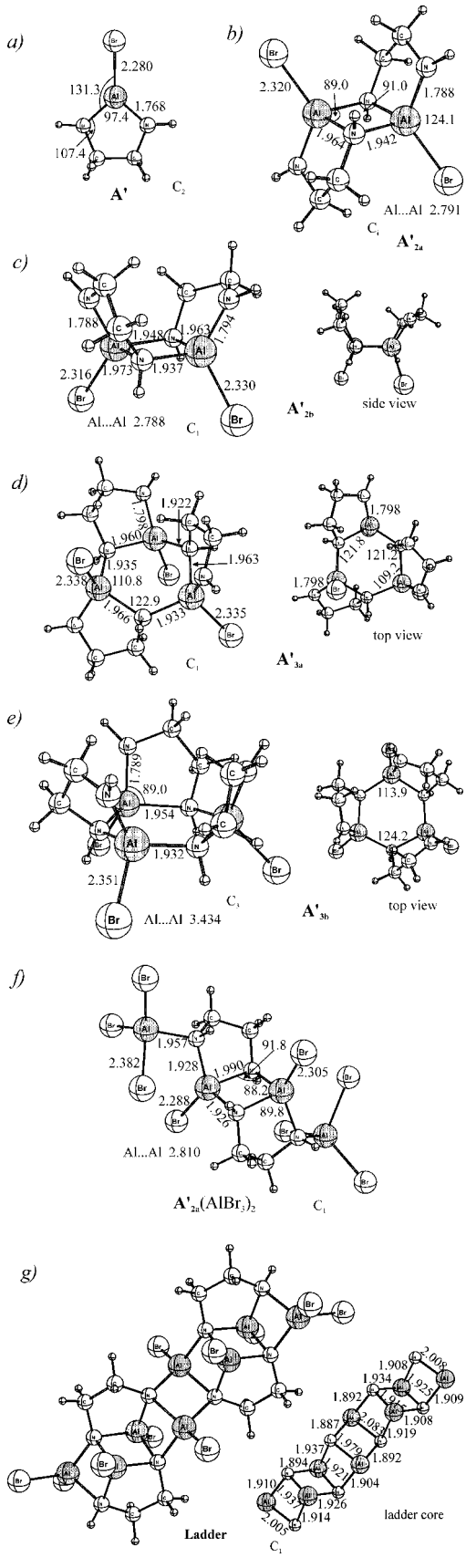

Figure 3. Optimized structures of amido compounds $\mathbf{A'}_n$ (B3LYP/LANL2DZ(d,p) level of theory): (a) ring isomer of monomeric amido imino compound **A′**; (b) *trans*-ring dimer $\mathbf{A'}_{\mathbf{2a}}$; (c) *cis*-ring dimer $\mathbf{A'}_{\mathbf{2b}}$; (d) *trans*-ring trimer $\mathbf{A'}_{\mathbf{3a}}$; (e) *cis*-ring trimer $\mathbf{A'}_{\mathbf{3b}}$; (f) Lewis acid-stabilized dimer $\mathbf{A'}_{\mathbf{2a}}(AlBr_3)_2$; (g) ladder-type structure **L**. All distances are in angstroms and all angles in degrees.

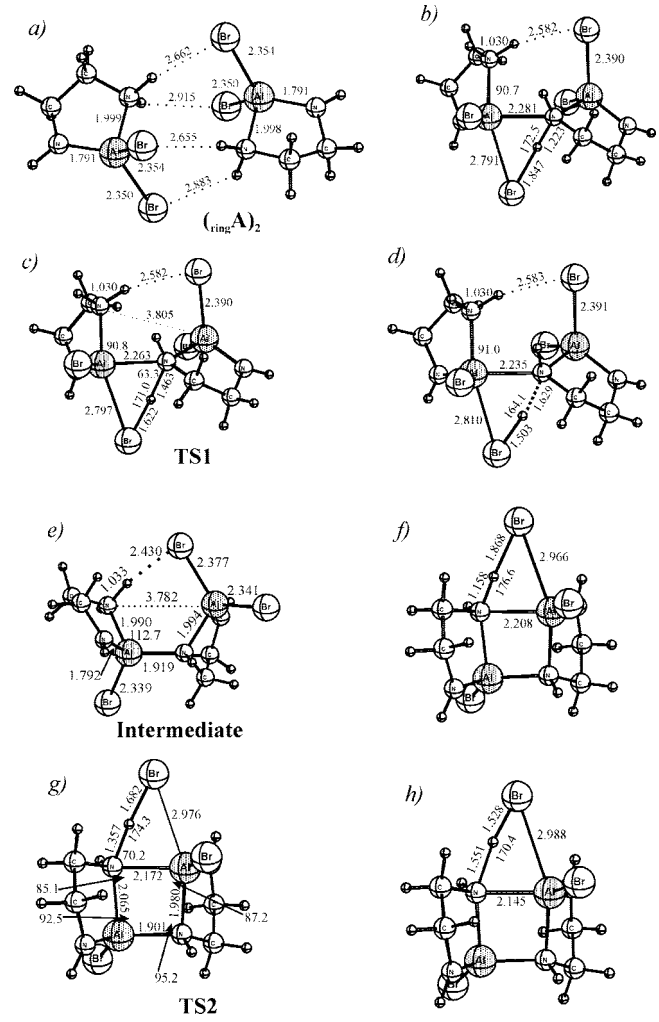

Figure 4. Structures related to the intermolecular HBr elimination pathway (B3LYP/LANL2DZ(d,p) level of theory): dimer $(\mathbf{_{ring}A})_2$ (a), transition state **TS1** for the first HBr elimination (c), and structures along the intrinsic reaction path for the reverse (b) and forward (d) directions; intermediate (e), transition state **TS2** for the second HBr elimination (g), and structures along the intrinsic reaction path for the reverse (f) and forward (h) directions. All distances are in angstroms and all angles in degrees.

supported amido compound $Br_2\overline{AlNHC_2H_4NH_2}$ ($\mathbf{_{ring}A}$) after HBr elimination. The species $\mathbf{_{ring}A}$ was experimentally detected by mass spectrometry as a decomposition product of the Al_2Br_6en complex and was found to be quite stable according to theoretical computations.[11] The analogous intramolecular DA-supported amido compounds $\overline{AlX_2(CH_2)_3NMe_2}$ (X = Cl, Br) were prepared by J. Müller. Their high-temperature thermolysis was experimentally investigated by the matrix isolation technique.[22]

A comparison of the thermodynamic characteristics for the different processes starting from $\mathbf{_{ring}A}$ is given in Table 2. The gas-phase dimerization of $\mathbf{_{ring}A}$ (process 1) is not favorable above 210 K due to entropy.[11] The dissociation of the donor−acceptor bond in $\mathbf{_{ring}A}$ with conversion into $\mathbf{_{chain}A}$ (process 2) is endothermic and is accompanied only by a small entropy gain. In contrast, HBr elimination with formation of monomeric **A′** (process 3) is accompanied by a significant entropy increase and becomes thermodynamically favorable above 1000 K. Note that the alternative HBr elimination reaction with formation of $\mathbf{I_a}$ (process 4) is energetically very unfavorable. Thus, HBr elimination is expected as a primary process

TABLE 2: Thermodynamic Characteristics for the Gas-Phase Reactions Starting from $_{ring}$A[a]

N	process	$\Delta H°_{298}$, kJ mol^{-1}	$\Delta S°_{298}$, J mol^{-1} K^{-1}	$\Delta G°_{298}$, kJ mol^{-1}	$T_{K=1}$, K
1[b]	$_{ring}$**A** ⇄ $^1/_2$**A$_2$**	−16.4	−78.6	7.0	209
2[b]	$_{ring}$**A** ⇄ $_{chain}$**A**	104.3	28.3	95.8	3682
3	$_{ring}$**A** ⇄ **A′$_a$** + HBr	217.4	133.0	177.8	1635
4	$_{ring}$**A** ⇄ **I$_a$** + HBr	423.1	140.4	381.2	3013
5	$_{ring}$**A** ⇄ $^1/_2$**A′$_{2a}$** + HBr	82.1	37.5	70.9	2187
6	$_{ring}$**A** ⇄ $^1/_4$**I$_4$** + HBr	116.8	9.5	113.9	12318
7	$_{ring}$**A** ⇄ $^1/_6$**I$_6$** + HBr	99.5	−19.4	105.3	-[c]
8	$_{ring}$**A** + $AlBr_3$ ⇄ $^1/_4$**L** + 2.5HBr	135.8	18.4	130.3	7402
8_H	$_{ring}$**A_H** + AlH_3 ⇄ $^1/_4$**L_H** + 2.5H_2	−237.8	−31.3	−228.5	7593
9	$_{ring}$**A** ⇄ $^1/_8$**I′$_8$** + 1.5HBr	169.0	42.5	156.2	3976
10	$_{ring}$**A** ⇄ $^1/_6$**I′$_6$** + 2HBr	202.8	106.1	171.2	1912
10_H	$_{ring}$**A_H** ⇄ $^1/_6$**I′$_6$** + 2H_2	−107.3	57.3	−124.4	-[d]

[a] B3LYP/LANL2DZ(d,p) level of theory. [b] Data from ref 11. [c] $K \ll 1$ at all T. [d] $K \gg 1$ at all T.

SCHEME 2: Energetic Pathway for the Intramolecular (a) and Intermolecular (b) HBr Elimination from $_{ring}$A[a]

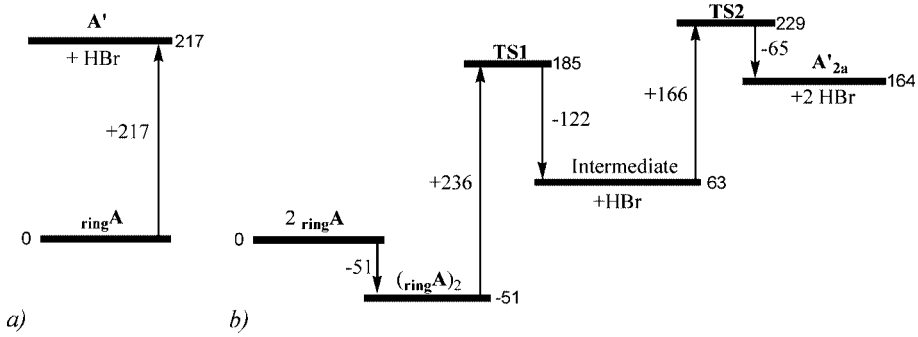

[a] Standard reaction enthalpies in kilojoules per mole.

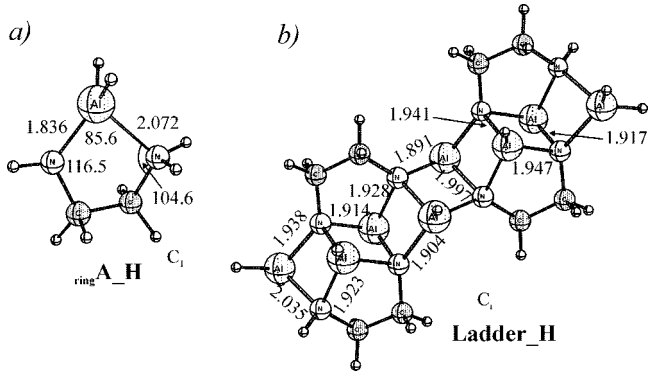

Figure 5. Optimized structures of hydrogen-substituted analogues (B3LYP/LANL2DZ(d,p) level of theory): (a) $_{ring}$**A_H**; (b) ladder-type structure **L_H**. All distances are in angstroms and all angles in degrees.

of $_{ring}$**A** destruction at high temperatures, followed by the very favorable dimerization of **A′**. The thermodynamic analysis shows that the overall formation of dimeric **A′$_{2a}$** from $_{ring}$**A** in the gas phase (process 5) is endothermic by 80 kJ per mole of $_{ring}$**A**. Thus, formation of **A′$_{2a}$** is the least endothermic process among the HBr elimination reactions (Table 2).

We have addressed the mechanism of the HBr elimination from $_{ring}$**A**. Both intra- and intermolecular elimination pathways have been considered. Our attempts to optimize the transition state (TS) for the intramolecular HBr elimination from $_{ring}$**A** were unsuccessful. By analogy with similar theoretical findings for the intramolecular HCl elimination from the Cl_3MNH_3 adducts,[24] the activation energy of the intramolecular HBr elimination from $_{ring}$**A** is not expected to be much larger than the reaction energy even if a transition state actually exists.[24a] In such a case the endothermicity of the reaction (217 kJ mol^{-1}) may be taken as an estimation of the corresponding activation energy.[24b]

We have located two transition states (**TS1** and **TS2**) for the intramolecular HBr elimination of HBr starting from two molecules of $_{ring}$**A**. To verify that the obtained transition states are indeed connecting source compounds and reaction products, we have performed intrinsic reaction coordinate scans of the PES. Optimized structures of the source dimer ($_{ring}$**A**)$_2$, **TS1**, intermediate compound, **TS2**, and selected geometries along the intrinsic reaction path in the forward and backward directions are given in Figure 4. Both **TS1** and **TS2** are of the late TS type, featuring relatively short Al−N distances of 2.263 and 2.172 Å, suggesting that formation of the new Al−N bond is basically finished. The Al−Br−H−N fragment in the TS is essentially planar with very long Al···Br distances and a nearly linear N···H···Br arrangement. Dimeric ($_{ring}$**A**)$_2$, **TS1**, and the resulting intermediate structure (Figure 4a,c,e) are additionally stabilized by intermolecular H···Br contacts of about 2.43−2.66 Å, which is a starting point for the elimination of the second HBr molecule.

The energetic profile of the intra- and intermolecular HBr elimination pathways from $_{ring}$**A** is presented in Scheme 2. Transition states for the intermolecular pathway lie relatively high in energy (185 and 229 kJ mol^{-1} for **TS1** and **TS2**, respectively, relative to the two $_{ring}$**A** molecules), which is comparable to the overall endothermicity of the intramolecular HBr elimination of 217 kJ mol^{-1}.

The generation of higher oligomers from $_{ring}$**A** is slightly more endothermic. The generation of imino tetramer **I$_4$** and imino hexamer **I$_6$** from $_{ring}$**A** in the gas phase (all values are given per mole of $_{ring}$**A**) is endothermic by 116 and 100 kJ mol^{-1}, respectively (processes 6 and 7). Formation of a ladder-type structure (process 8) is endothermic by 136 kJ mol^{-1}, and

formation of $\mathbf{I'_8}$ and $\mathbf{I'_6}$ (processes 9 and 10) is endothermic by 169 and 205 kJ mol^{-1}.

Our computational results suggest that all HBr elimination processes in *the gas phase* are thermodynamically not allowed. Note that HBr elimination was experimentally observed upon heating of the M_2X_6en complexes (M = Al, Ga; X = Cl, Br, I).[11] We conclude that HBr elimination reactions take place in the condensed phase after melting of the complex. The resulting products after HBr elimination are viscous oils that are likely to have a polymeric nature.

The fact that both inter- and intramolecular HBr elimination processes are strongly endothermic in the gas phase (Table 2) dovetails with the endothermicity of the hydrogen halide elimination reactions in general.[12] In contrast, substitution of halogen atoms by hydrogen results in exothermic H_2 elimination.[19] The exothermicity of H_2 and methane elimination reactions was also noted for the generation of the GaN imino oligomers.[23] One can expect that using hydride and organoaluminum derivatives as starting materials will make the formation of oligomers, such as ladders **L** and handled cages $\mathbf{I'_6}$, thermodynamically feasible.

To confirm this statement, we optimized the hydrogen-substituted analogues of $_{\mathrm{ring}}\mathbf{A}$ and ladder **L**. Their optimized structures are given in Figure 5. Comparison of the thermodynamic characteristics for HBr (processes 8 and 10) and H_2 (processes 8_H and 10_H) elimination reactions reveals that formation of both ladder and cage compounds is exothermic in the case of hydrogen elimination. Reaction 10_H is thermodynamically allowed at all temperatures. Although reaction 10_H in the gas phase is slightly unfavorable by entropy, formation of species with high oligomerization degrees in the condensed phase is expected to be thermodynamically favorable for hydrogen-substituted and metallorganic derivatives. Theoretical studies on the structures and stability of new members of the "handled" aluminum−nitrogen oligomers and their conversion to bulk AlN are currently under way.

4. Conclusion

Determination of the structures and thermodynamic properties of two series of ring and cage oligomer compounds has been performed at the B3LYP/LANL2DZ(d,p) level of theory. A variety of different oligomeric structures which result during HBr elimination from the $AlBr_3$en complex have been theoretically explored. Structures which feature intramolecular donor−acceptor bonds are predicted to be more stable compared to their unstabilized isomers. Thus, formation of the organic handles (five-membered $\overline{\mathrm{Al-N-C-C-N}}$ rings) plays an essential role in the stabilization of the imino structures.

In contrast to amido species, the stability of the imino compounds increases with an increase of the oligomerization degree *n*, which points out the possibility of polymer formation. Substitution of bromide by hydrogen results in the exothermic generation of both "handled" cages and "balustrade" ladder compounds. These compounds provide a viable alternative to the 2D structures theoretically considered by Himmel.[9] Further theoretical and experimental studies in this direction are highly desirable and expected to be very promising.

Acknowledgment. A.Y.T. is grateful to INTAS for the YS05-109-4196 fellowship. C.T. is grateful to the Vietnamese Government for a full scholarship during five years of undergraduate study in Russia. Excellent service of the MARC computer cluster of Philipps-University Marburg and computer cluster of St. Petersburg State University is gratefully acknowledged.

Supporting Information Available: Table with total energies, sum of electronic and thermal enthalpies, and standard entropies for the studied compounds. This material is available free of charge via the Internet at http://pubs.acs.org.

References and Notes

(1) (a) Jones, A. C.; O'Brien, P. *CVD of Compound Semiconductors. Precursor Synthesis, Development and Applications*; VCH: Weinheim, Germany, 1997. (b) DenBaars, S. P. *Proc. IEEE* **1997**, *85*, 1740. (c) *N-Containing III-V Semiconductors: Fundamentals and Applications. European Materials Research Society Symposia Proceedings, 136, Elsevier, Amsterdam, 2003*; Chen, W. M., O'Reilly, E., Forchel, A., Tu, C. W., Eds. *Solid-State Electron.* **2003**, *47*, 385−592.

(2) Pierson, H. O., Ed. *Handbook of Chemical Vapor Deposition: Principles, Technology and Applications*, 2nd ed.; William Andrew Publishing, LLC: New York, 2000; 482 pp.

(3) (a) Stringfellow, G. B. *Organometallic Vapor Phase Epitaxy: Theory and Practice*; Academic Press: New York, 1989. (b) Stringfellow, G. B. *Organometallic Vapor Phase Epitaxy*, 2nd ed.; Academic Press: New York, 1998.

(4) Zheng, Z.; Yang, Y.; Yu, B.; Song, X.; Li, X. *ACS Nano* **2008**, *2*, 134.

(5) Schulz, S.; Bauer, T.; Hoffbauer, W.; Schmedt auf der Günne, J.; Doerr, M.; Marian, C. M.; Assenmacher, W. *J. Solid State Chem.* **2008**, *181*, 530.

(6) Koyama, S.; Takeda, H.; Tsugosho, T.; Watari, K.; Sugahara, Y. *J. Ceram. Soc. Jpn.* **2006**, *114*, 563.

(7) Mori, Y.; Sugahara, Y. *J. Ceram. Soc. Jpn.* **2006**, *114*, 461.

(8) Mori, Y.; Kumakura, Y.; Sugahara, Y. *J. Organomet. Chem.* **2006**, *691*, 4289.

(9) Himmel, H.-J. *ChemPhysChem* **2005**, *6*, 706.

(10) Timoshkin, A. Y.; Schaefer, H. F. *Chem. Rec.* **2002**, *2*, 319.

(11) Trinh, C.; Timoshkin, A. Y.; Matweev, S. M.; Misharev, A. D. *J. Organomet. Chem.* **2007**, *692*, 2822.

(12) Trinh, C.; Timoshkin, A. Y.; Frenking, G. *ChemPhysChem* **2007**, *8*, 425.

(13) (a) Timoshkin, A. Y. *Coord. Chem. Rev.* **2005**, *249*, 2094. (b) Timoshkin, A. Y.; Schaefer, H. F. *J. Phys. Chem. C* **2008**, *112*, 13816.

(14) Frisch, M. J.; Trucks, G. W.; Schlegel, H. B.; Scuseria, G. E.; Robb, M. A.; Cheeseman, J. R.; Montgomery, J. A., Jr.; Vreven, T.; Kudin, K. N.; Burant, J. C.; Millam, J. M.; Iyengar, S. S.; Tomasi, J.; Barone, V.; Mennucci, B.; Cossi, M.; Scalmani, G.; Rega, N.; Petersson, G. A.; Nakatsuji, H.; Hada, M.; Ehara, M.; Toyota, K.; Fukuda, R.; Hasegawa, J.; Ishida, M.; Nakajima, T.; Honda, Y. ; Kitao, O.; Nakai, H.; Klene, M.; Li, X.; Knox, J. E.; Hratchian, H. P.; Cross, J. B.; Bakken, V.; Adamo, C.; Jaramillo, J.; Gomperts, R.; Stratmann, R. E.; Yazyev, O.; Austin, A. J.; Cammi, R.; Pomelli, C.; Ochterski, J. W.; Ayala, P. Y.; Morokuma, K.; Voth, G. A.; Salvador, P.; Dannenberg, J. J.; Zakrzewski, V. G.; Dapprich, S.; Daniels, A. D.; Strain, M. C.; Farkas, O.; Malick, D. K.; Rabuck, A. D.; Raghavachari, K.; Foresman, J. B.; Ortiz, J. V.; Cui, Q.; Baboul, A. G.; Clifford, S.; Cioslowski, J.; Stefanov, B. B.; Liu, G.; Liashenko, A.; Piskorz, P.; Komaromi, I.; Martin, R. L.; Fox, D. J.; Keith, T.; Al-Laham, M. A.; Peng, C. Y.; Nanayakkara, A.; Challacombe, M.; Gill, P. M. W.; Johnson, B.; Chen, W.; Wong, M. W.; Gonzalez, C.; Pople, J. A. *Gaussian03*, revision B.05; Gaussian, Inc.: Wallingford, CT, 2004.

(15) Becke, A. D. *J. Chem. Phys.* **1993**, *98*, 5648.

(16) Lee, C.; Yang, W.; Parr, R. G. *Phys. Rev. B* **1988**, *37*, 785.

(17) Hay, P. J.; Wadt, W. R. *J. Chem. Phys.* **1985**, *82*, 270.

(18) Timoshkin, A. Y.; Suvorov, A. V.; Bettinger, H. F.; Schaefer, H. F. *J. Am. Chem. Soc.* **1999**, *121*, 5687.

(19) Timoshkin, A. Y.; Schaefer, H. F. *Inorg. Chem.* **2004**, *43*, 3080.

(20) Timoshkin, A. Y. *Chemtracts: Inorg. Chem.* **2005**, *18*, 637.

(21) Timoshkin, A. Y.; Suvorov, A. V.; Schaefer, H. F. *Russ. J. Gen. Chem.* **2001**, *71*, 8.

(22) Müller, J.; Wittig, B. *Eur. J. Inorg. Chem.* **1998**, 1807.

(23) Timoshkin, A. Y.; Schaefer, H. F. *J. Am. Chem. Soc.* **2004**, *126*, 12141.

(24) (a) Okamoto, Y. *J. Cryst. Growth* **1998**, *191*, 405. (b) Timoshkin, A. Y.; Bettinger, H. F.; Schaefer, H. F. *Inorg. Chem.* **2002**, *41*, 738.

JP805904E